IUBMB *Life*, 63(12): 1101–1110, December 2011

Research Communication

Benzothiophene Carboxamide Derivatives as Inhibitors of *Plasmodium falciparum* Enoyl-ACP Reductase

Tanushree Banerjee[1], Shailendra Kumar Sharma[2]*, Neha Kapoor[1]*, Vishnu Dwivedi[1], Namita Surolia[3] and Avadhesha Surolia[1]

[1]*National Institute of Immunology, New Delhi, India*

[2]*Molecular Biophysics Unit, Indian Institute of Science, Bangalore, India*

[3]*Jawaharlal Nehru Centre for Advanced Scientific Research, Jakkur, Bangalore, India*

Summary

Benzothiophene derivatives like benzothiophene sulphonamides, biphenyls, or carboxyls have been synthesized and have found wide pharmacological usage. Here we report, bromo-benzothiophene carboxamide derivatives as potent, slow tight binding inhibitors of *Plasmodium* enoyl-acyl carrier protein (ACP) reductase (PfENR). 3-Bromo-*N*-(4-fluorobenzyl)-benzo[b]thiophene-2-carboxamide (compound 6) is the most potent inhibitor with an IC_{50} of 115 nM for purified PfENR. The inhibition constant (K_i) of compound 6 was 18 nM with respect to the cofactor and 91 nM with respect to crotonoyl-CoA. These inhibitors showed competitive kinetics with cofactor and uncompetitive kinetics with the substrate. Thus, these compounds hold promise for the development of potent antimalarials.
IUBMB *Life*, 63(12): 1101–1110, 2011

Keywords bromo-benzothiophene; benzothiophene carboxamide; antimalarials; *Plasmodium*.

Abbreviations FAS, fatty acid synthase; GPI, glycosylphosphatidylinositol; PfENR, *Plasmodium falciparum* enoyl-ACP reductase; NADH, nicotinamide adenine dinuleotide reduced; ADH, alcohol dehydrogenase.ACP: Acyl Carrier Protein DCC- Dicyclohexyl Carbodiimide HoBt-1-Hydroxybenzotriazole DMF-Dimethy formamide ES-MS-Electron Spray Mass Spectrometry DMSO: DimethylSulphonyl Oxide SDS/PAGE-Sodium Dodecyl Sulphate/ Polyacrylamide Gel Electrophoresis PDB: Protein Database

INTRODUCTION

Socioeconomic burden of malaria is increasing due to the emergence of resistance towards the mainstay antimalarials (*1–4*). There are variations in the frequency of resistance development towards the existing drugs, which depends on the genetic traits of both the host and the pathogen. Environmental factors also play a deterministic role in the development of resistance (*5*). Approximately 40% of world's population is under threat of malaria, which includes the countries in Asia, Africa, Latin America, and South Pacific (*6*). Its causative agent is the apicomplexan protozoan *Plasmodium*. The genus *Plasmodium* has four species: *malariae*, *vivax*, *falciparum*, and *ovale*, which infect humans. Recently, the monkey malaria parasite *Plasmodium knowlesi* was also shown to infect humans. Among the human malaria parasites, *Plasmodium falciparum* causes the most fatal form of malaria *viz*. cerebral malaria. In the absence of a vaccine and complete control on transmission vector, it is imperative to develop new antimalarials.

Current insights on the *Plasmodium's* metabolome have uncovered different targets for the development of novel antimalarials. Also, fatty acids biosynthesis enzymes are one of the important targets. Tremendous proliferative potential of *Plasmodium* makes it essentially depend on abundant supply of fatty acids. Fatty acids are required for membrane synthesis, lipid biogenesis and glycosylphosphatidylinositol (GPI) anchors of its transmembrane proteins. In the case of *Plasmodium*, *de novo* synthesis of fatty acids occurs by type II fatty acid synthase (FAS), which is fundamentally different from type I FAS system of humans (*7–11*). Using inhibitors (*12*) and type II FAS enzyme knock-out parasite lines (*13*), it has recently been shown to be indispensable for liver-stage parasite development which further strengthens its significance in the parasite biology.

In brief, the fatty acid synthesis starts with the formation of malonyl-acyl carrier protein (ACP) by malonyl-CoA ACP transacylase (FabD). Malonyl-ACP undergoes decarboxylative con-

Additional Supporting Information may be found in the online version of this article.

*These authors contributed equally to this work.

Address correspondence to: Avadhesha Surolia, National Institute of Immunology, Aruna Asaf Ali Marg, New Delhi 11067, India. E-mail: surolia@nii.res.in

Received 22 June 2011; accepted 7 July 2011

ISSN 1521-6543 print/ISSN 1521-6551 online
DOI: 10.1002/iub.553

densation with acetyl-CoA by the enzyme β-ketoacyl-ACP synthase III (FabH) or acyl-malonyl-ACP condensing enzyme (FabB or Fab F), respectively. This reaction is followed by nicotinamide adenine dinucleotide phosphate reduced (NADPH) dependent reduction, which is catalyzed by β-ketoacyl-ACP reductase (FabG) forming β-hydroxy butyryl-ACP. β-Hydroxy butyryl-ACP is then dehydrated to *trans*-2-butyryl-ACP (crotonoyl-ACP) by β-hydroxy acyl-ACP dehydratases (Fab A or Fab Z). The last step is the nicotinamide adenine dinuleotide reduced (NADH) dependent reduction, of the enoyl-ACP catalyzed by enoyl-ACP reductase (FabI) forming butyryl-ACP. Repetition of the elongation cycle 6–7 times yields a long acyl chain covalently linked to ACP. *Plasmodium* enoyl-ACP reductase (PfENR) catalyzes the deterministic step of the elongation cycle and therefore, has emerged as an important drug target (*9, 14–18*).

Benzothiophene derivatives are heterocyclic aromatic compounds which have found extensive pharmacologic applications. Benzothiophene biphenyl derivatives have been shown to have inhibitory activity against tyrosine phosphatase1B and antihyperglycaemic properties (*19*). Raloxifene and arzoxifene are benzothiophene derivatives which act as selective estrogen receptor modulators of clinical value in postmenopausal osteoporosis, treatment of breast cancer, and potentially in hormone replacement therapy (*20, 21*). Benzothiophene class of compounds act as antagonist to retinoid X receptors, activator of a TRPV4 (Transient Receptor Potential Vallinoid subtype IV) channel (*22*) and also have antitumor properties (*23*).

PfENR which is an important antimalarial drug target is effectively inhibited by bromo-benzothiphene carboxamide compounds. Hence, these compounds hold promise for the development of potent antimalarials.

CHEMISTRY

Syntheses were performed according to the generic pathway depicted in Scheme 1. Bromobenzo[b]thiophene-2-carboxylic acid [**2**] was coupled with different commercially available arylalkyl amines to obtain the target compounds **4–9** using activated ester of bromobenzo[b]thiophene-2-carboxylic acid (*24*). In syntheses, compounds **6** and **7** were treated with allyl bromide at 60 °C for 48 h to obtain 3-bromo-*N*-(4-fluorobenzyl)-*N*-(prop-2-en-1-yl)-benzo[b]thiophene-2-carboxamide **10** and 3-bromo-*N*-(prop-2-en-1-yl)-*N*-[4-(trifluoromethyl)benzyl]-1-benzo[b]thiophene-2-carboxamide **11**, respectively (*25*). Purity of each compound was 97–99%.

SYNTHESIS OF COMPOUNDS

General

All solvents (synthetic grade) were purchased from Merck Schuchardt and purified before use. Benzothiophene-2-carboxylic acid, benzyl amine, 4-methoxy benzyl amine, 4 fluorobenzyl amine, 4-(trifluoromethyl)-benzyl amine, 2-phenyl ethyl amine, and 1-naphthalene-methyl amine were purchased from Aldrich. Melting points were determined with the Barnstaed electrothermal apparatus and are uncorrected. Mass analysis was done using Perkin Elmer API 165 Sciex mass spectrometer. ^{1}H and ^{13}C NMR spectral analyses were performed on Bruker DRX 400 spectrometer with tetra-methylsilane as the internal standard (δ ppm). The following abbreviations were used to explain the multiplicities: s, singlet; d, doublet; t, triplet; dd, double doublet; m, multiplet, br, broad. Solvents and reagents were purified according to standard laboratory techniques.

General Procedure for Synthesis of Compounds 4–9. To a cooled mixture (ice bath) of 3-bromobenzo[b]thiophene-2-carboxylic acid (**2**) (0.60 g, 2.33 mmol), corresponding arylalkyl amine (3.12 mmol), dicyclohexyl carbodiimide (DCC) (0.48 g, 2.33 mmol), and hydroxybenzotriazole (HOBt) (0.31 g, 2.29 mmol) was added anhydrous dimethyl formamide (DMF) (15 mL). The reaction mixture was stirred overnight at room temperature under nitrogen atmosphere till completion of the reaction. The reaction mixture was vacuum filtered to remove precipitated dicyclohexylurea. The filtrate was then evaporated under reduced pressure to give dark oil which was dissolved in ethyl acetate (20 mL) and then refiltered. The filtrate was vacuum evaporated and the oily residue was purified by column chromatography (30% ethyl acetate: hexane). To prevent the product from crystallization in the column, a short column was run under pressure to yield the target compounds (Scheme 1).

N-Benzyl-3-bromobenzo[b]thiophene-2-carboxamide(4). Crystalline colorless solid (0.78 g, 98%). M.p. 115–117 °C. Electron spray mass spectrometry (ES-MS) *m/z*: Calcd for $C_{16}H_{12}BrNOS$: 346.24 [M^+]; Obsd 346. ^{1}H NMR ($CDCl_3$, 300 MHz): 4.72 (d, 2H, CH_2), 7.31–7.45 (m, 5H, ArH benzyl), 7.48 (m, 2H, ArH), and 7.83 (dd, 2H, ArH). ^{13}C NMR: 44.5, 106.6, 122.9, 124.7, 125.8, 127.9, 128.0, 129.1, 137.7, 138.6, 138.7, and 161.1.

3-Bromo-N-(4-methoxybenzyl)-benzo[b]thiophene-2-carboxamide(5). Crystalline colorless, solid (0.85 g, 3.30 mmol). Mp. 123–124 °C. ES-MS *m/z*: Calcd for $C_{17}H_{14}BrNO_2S$: 376.27 [M^+]; Obsd 376.26. ^{1}H NMR ($CDCl_3$, 300 MHz): 3.80 (s, 3H, OMe), 4.65 (d, 2H, CH_2), 6.91 (m, 2H), 7.34 (m, 2H), 7.46 (m, 2H, ArH), and 7.83 (d, 2H, ArH). ^{13}C NMR: 44.0, 55.5, 106.6, 114.4, 122.9, 124.7, 125.7, 125.7, 129.4, 135.1, 138.7, 159.4, and 161.0.

3-Bromo-N-(4-fluorobenzyl)-benzo[b]thiophene-2-carboxamide(6). M.p. 120–125 °C. ES-MS *m/z*: Calcd for $C_{16}H_{11}BrNOSF$; 364.23 [M^+]; Obsd 364.20. ^{1}H NMR ($CDCl_3$, 300 MHz) 4.70 (d, 2H), 7.45 (m, 2H, ArH) 7.83 (dd, 2H, ArH) 7 (m, 2H), and 7.36 (m, 2H). ^{13}C NMR 44.0, 106.6, 125.7, 124.7, 123.9, 124.5, 130, 138.7, 163.5, and 161.0.

3-Bromo-N-[4-(trifluoromethyl)benzyl]-benzo[b]thiophene-2-carboxamide(7). Mp. 128–130 °C. ES-MS *m/z*: Calcd for $C_{17}H_{11}BrF_3NOS$ 414.24 [M^+], Obsd 414. ^{1}H NMR ($CDCl_3$, 300 MHz): 4.70 (d, 2H), 7.47 (m, 2H, ArH), 7.12 (m, 2H), and 7.38 (m, 2H). ^{13}C NMR 44.0, 106.6, 125.7, 124.7, 123.9, 124.5, 130, 138.7, and 161.0.

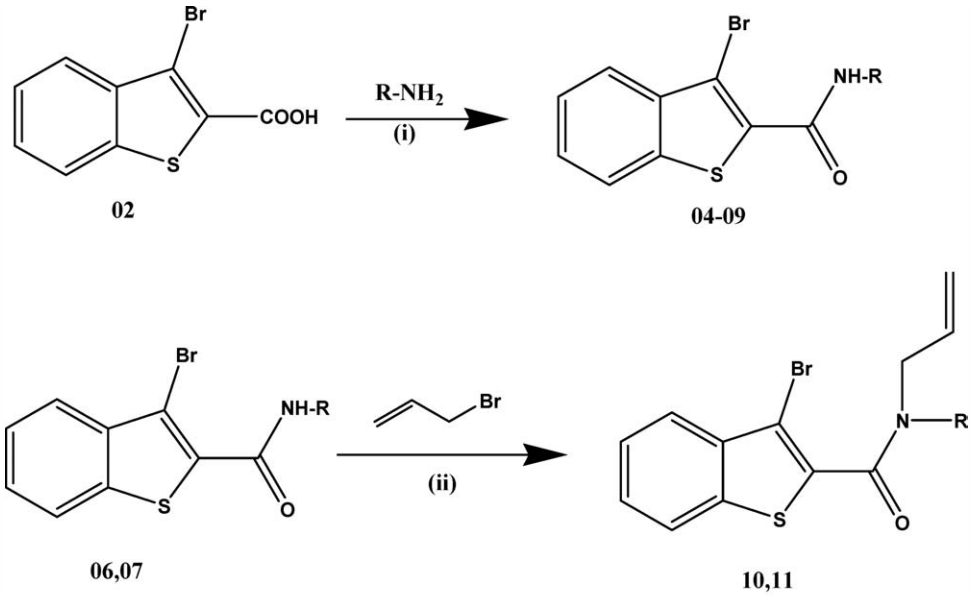

Compound	R
04	benzyl
05	4-methoxybenzyl
06	4-fluorobenzyl
07	4-trifluorobenzyl
08	2-phenylethyl
09	naphthalene-1-ylmethyl
10	4-fluorobenzyl
11	4-trifluorobenzyl

Scheme 1. Synthesis of benzothiophene arylalkylamide derivatives. (i) Anhyd DMF, arylalkyl amine, DCC, HOBt, overnight (stirring under N2 atmosphere at RT) (ii) Anhyd. THF, NaH/60 °C/30 min, CH_2=CHCH2Br, 48 h (heat with stirring). Conditions: (i) Br_2/CH_3COONa, (ii) $SOCl_2$/Toluene/Pyridine/3 h, (iii) activated ester of compound 2 and arylalkyl amines, and (iv) allyl bromide.

3-Bromo-N-(2-phenylethyl)-benzo[b]thiophene-2-carboxamide (8). Colorless solid. ES-MS *m/z*: Calcd for $C_{17}H_{14}BrNOS$ 360.27 [M^+]; Obsd 360. ^{1}H NMR ($CDCl_3$, 300 MHz): 3.5 (d, 2H), 3.2 (d, 2H), 7.47 (m, 2H, ArH) 7.12 (m, 2H), and 7.38 (m, 2H).^{13}C NMR 42.9, 35.5, 106.6, 125.7, 124.7, 123.9, 124.5, 130, 138.7, and 161.0.

3-Bromo-N-(naphthalen-1-ylmethyl)-benzo[b]thiophene-2-carboxamide(9). Colorless solid. ES-MS *m/z*: Calcd for $C_{20}H_{14}BrNOS$ 396.30 [M^+]; Obsd 396. ^{1}H NMR ($CDCl_3$, 300 MHz): 4.9 (d, 2H), 7.47 (m, 2H, ArH), 7.12 (m, 2H), 7.38 (m, 2H), 7.1 (m, 2H), 7.3 (m, 2H), and 7.6 (s, 1H). ^{13}C NMR (75 MHz): 44.0, 125.7, 124.7, 123.9, 124.5, 127.4, 127.5, 128.3, 128.2, 130, 138.7, and 161.0.

General Procedure for Synthesis of 10 and 11. To a solution of **06** or **07** (1 mmol) in dry THF was added NaH and heated at 60 °C for 30 min. Allyl bromide (1.2 mmol) was added to the resulting mixture and heated at 70 °C for 24 h. NaH and allyl bromide were further added to the reaction mass and maintained at 70 °C for another 24 h. The solvent was vacuum evaporated, and the residue was extracted with diethyl ether, washed with brine, dried and evaporated under reduced pressure. The residue was purified by column chromatography (2% EtOAc-hexane; Scheme 1)

3-Bromo-N-(4-fluorobenzyl)-N-(prop-2-en-1-yl)-benzo[b]thiophene-2-carboxamide (10). Colorless solid. ES-MS *m/z*: Calcd for $C_{19}H_{15}BrFNOS$ 404.30 [M^+]; Obsd 403.0. ^{1}H NMR ($CDCl_3$,

300 MHz): 4.70 (d, 2H), 5.18 (d, 2H), 7.45 (m, 2H, ArH), 7.83 (2H, ArH), 7 (m, 2H), and 7.36 (m, 2H). ^{13}C NMR (75 MHz): 58.0, 106.6, 125.7, 124.7, 123.9, 124.5, 130, 138.7, 163.5, 136, 137.5, and 161.0.

3-Bromo-N-(prop-2-en-1-yl)-N-[4-(trifluoromethyl)benzyl]-1-benzo[b]thiophene- 2-carboxamide (11). Colorless solid. ES-MS *m/z*: Calcd for $C_{20}H_{15}BrF_3NOS$ 454.30 [M^+]; Obsd 454.4. ^{1}H NMR ($CDCl_3$, 300 MHz): 4.70 (d, 2H), 5.18 (s, 2H), 7.47 (m, 2H, ArH) 7.12 (m, 2H), and 7.38 (m, 2H). ^{13}C NMR 58.0, 106.6, 125.7, 124.7, 123.9, 124.5, 130, 136.4, 138.7, 142.2, and 161.0.

EXPERIMENTAL

Materials for PfENR Preparation and Enzyme Assay

Media components were purchased from Hi-media (Delhi, India). β-NADH, crotonoyl CoA, imidazole, dimethylsulphonyl oxide (DMSO), and sodium dodecyl sulphate/polyacrylamide gel electrophoresis (SDS/PAGE) reagents were bought from Sigma. All other chemicals were of analytical grade.

Preparation of the Receptor and Ligand Molecules

The crystal structure of PfENR submitted to protein database (PDB) (PDB id: 1UH5) by Pidugu et al. (*26*) was used for docking simulations. Hydrogens were added and energy-minimized using molecular modelling program Molecular Operating Environment (MOE) (*27*). The three-dimensional coordinates were then converted to mol2 format with MMFF94 charges using the MOE suite of programs. Receptor was prepared for docking by Protonate three dimensional Macromolecular Protonation State Assignment tool part of MOE suite and partial charge of the receptor were fixed. Ligand molecules were prepared using MOE-builder tool, a part of MOE suite and were subjected to energy minimization to a gradient of 0.0001 using dielectric constant of 1 and partial charges were calculated by MMF94x force field.

Docking experiments were executed using molecular docking structure-based design tool, a part of MOE suite 2009.10. The compounds were docked by default nonstochastic Triangular Matcher Placement method using the London dG scoring, followed by force field refinement using default configurations of docking simulations. Each ligand was docked in the receptor protein and top 100 conformations were retained. Docked complex with least energy was chosen for ligand protein contact analysis.

The ligand receptor complex with compounds **6** and **7** along with NAD were subjected to 15 cycles of energy minimization. These ligand receptor protein complexes were further subjected to LPC/CSU software for detailed analysis of the interatomic contacts (Supporting Information Tables 1–3) (*28*).

Overexpression and Purification of PfFAS Enzymes

*Pf*ENR was overexpressed in *E. coli*BL-21(DE3) cells according to the earlier published protocol with the only difference that all buffers contained 10% glycerol (*29*). Purity of the enzyme was checked by SDS-PAGE. Purified enzyme was stored at −20 °C at a concentration of 3 mg/mL till further use. PfFabB/F, PfFabG, and PfFabZ were purified and assayed as described earlier (*30–32*).

Assay of PfFAS Enzymes

Enzyme assays and inhibition studies were performed on a UV-Vis spectrophotometer (Shimadzu UV 2450) at 25 °C in 20 mM Tris/HCl and 150 mM NaCl, pH 7.4 (*33*). The standard reaction mixture (100 μL) contained 200 μM crotonoyl-CoA, 100 μM NADH and 30 nM *Pf*ENR. All the inhibitors were dissolved in DMSO. 1% DMSO was used in the standard reaction mixture. The reaction proceeds by reduction of crotonoyl-CoA to butyryl-CoA with the oxidation of NADH to NAD^+ which is monitored at 340 nm (ε^{M}_{340} = 6220 M^{-1} cm^{-1}). PfFabB/F, PfFabG, and PfFabZ enzymes were assayed according to refs. *30–32*.

Purification and Assay of Aldose Reductase

Recombinant human aldose reductase was expressed, purified, and assayed as described in refs. *34* and *35*. The purified enzyme was assayed spectrophotometrically as described in detail in supporting information. Decrease in the absorption of NADPH at 340 nm was measured over a period of 4 min with DL-glyceraldehyde as the substrate. Inhibition of enzyme activity was monitored in the presence of compounds **6** and **7**.

Inhibition Studies of Alcohol Dehydrogenase

The activity of alcohol dehydrogenase (ADH) was measured as described previously (*36*). The assay mixture in 1 mL contained 76 mM sodium pyrophosphate-22 mM glycine buffer pH 8.0, 2.0 mM NA, 0.60 mM ethanol, and 0.01 μM alcohol dehydrogenase (Cat no. A-3263; Sigma). Appropriate blanks were used for corrections. The assay mixture was incubated at 37 °C and initiated by the addition of NAD at 37 °C. The change in the absorbance at 340 nm because of NAD reduction was followed in a Lamda35 spectrophotometer (Perkin–Elmer, Shelton).

Determination of IC_{50} Value for PfFAS Enzymes

IC_{50} values of the bromo-benzothiophene carboxamide class of compounds were determined for *Pf*FAS enzymes and aldose reductase by plotting the percent activity of *Pf*FAS versus logarithm of the concentration of these compounds and the data were analyzed by nonlinear regression method (*37, 38*).

Calculation of Dissociation Constants (K_i)

K_i of compound **6** was calculated with respect to NADH and crotonoyl-CoA in separate experiments. With respect to NADH, data were collected against two fixed concentrations of NADH (100 μM and 200 μM) while varying the concentration of **6** from 0 to 750 nM keeping crotonoyl-CoA concentration fixed at 200 μM. For K_i with respect to crotonoyl-CoA, data were collected against two fixed concentrations of crotonoyl-CoA (100 μM and 200 μM) and concentration of **6** was varied from

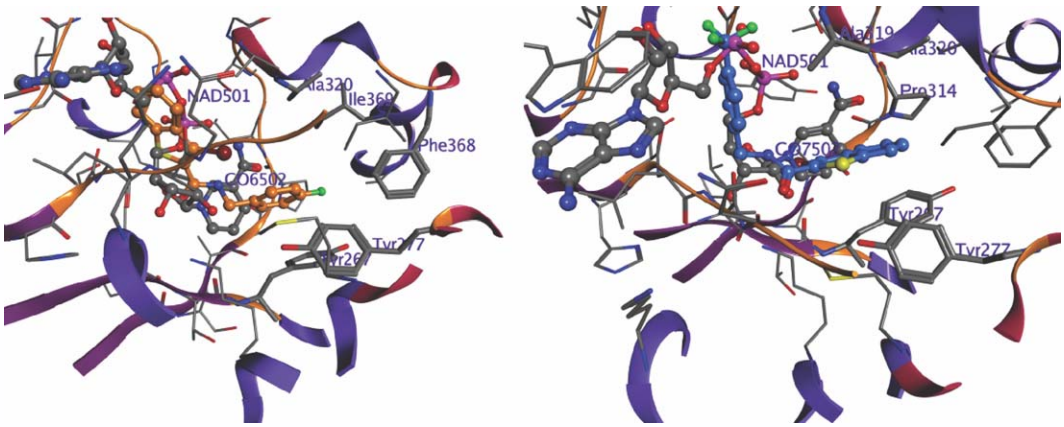

Figure 1. Compounds (a) **6** and (b) **7** docked with PfENR-NAD^+ complex. The inhibitors are shown in "Balls and Sticks." NAD and active-site residues are shown in sticks. Figures were generated using MOE v208.10.

0 to 750 nM, whereas NADH was kept constant. Data were analyzed by Dixon plot (*39*).

Potency Assays

Potency assays for inhibition of PfENR was designed as described earlier (*33*). The activity of purified PfENR was inhibited by addition of **6** (IC_{50} value) with and without preincubation time. Addition of (10 μM) **6** to the above reaction was shown to potentiate the inhibitory activity of **6**. First, the control reaction (a) was set as described earlier. The formation of NAD^+ was monitored at 340 nm. NAD^+ accumulation was observed to increase linearly with time. Reaction (b) contained compound **6**. Reaction (c) was set up with compound **6** but with a preincubation time of 20 min. In reaction (d) the enzyme was preincubated with both NAD^+ and compound **6**.

Determination of Association (k_5 or k_{on}) and Dissociation Rate Constants (k_6 or k_{off}) of Compounds 6 and 7 for PfENR

The association or isomerization rate constant (k_5) of compounds **6** and **7** with *Pf*ENR was determined separately by monitoring the onset of inhibition in the enzyme reactions. In the reaction mixture compounds **6** and **7** were added (0–750 nM) sequentially and the formation of NAD^+ was plotted against time by nonlinear regression method using Eq. (2a) discussed later to get k_{obs} for each concentration of compounds **6** and **7** used. The values of k_{obs} were fitted to Eq. (3) to get K_i, k_5, and k_6 values. The hyperbolic curve obtained clearly depicts the slow tight binding nature of inhibition (*40, 41*).

Evaluation of the Kinetic Data

Initial rate constants were determined using Dixon plot assuming the reaction to be competitive for compound **6** against NADH and uncompetitive for compound **7** against crotonoyl-CoA. The data were plotted using the following Dixon equations for competitive [Eq. (1a); ref. *39*] and uncompetitive kinetics [Eq. (1b); ref. *39*], respectively.

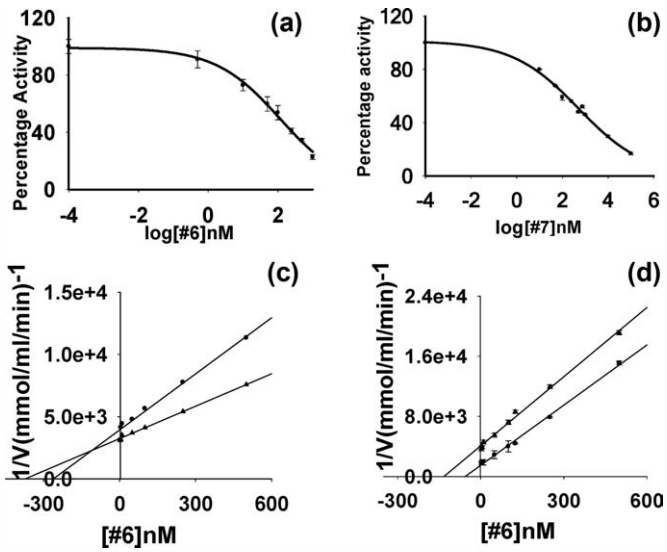

Figure 2. (a, b) Inhibition of PfENR at various concentration (0–1 μM) of compounds. The percentage activity was calculated from residual activity and was plotted against log concentration. (a) Compound **6** and (b) compound **7**. (c) Inhibition kinetics of compound **6** with respect to NADH. The effect of NADH on inhibition by compound **6** was determined using Dixon plot. 30 nM PfENR was assayed in the presence of 200 μM crotonoyl CoA and at two concentrations of NADH, 100 μM [▲], 150 μM [●] with various concentration of compound **6**. K_i of compound **6** was calculated from the X-intercept using equation for competitive kinetics. Each data point indicates three different data sets and the error bar indicates the standard deviation of the data. (d) Inhibition of PfENR by compound **6** with respect to crotonoyl CoA. PfENR was assayed at two fixed concentrations 200 μM [●] and 300 μM [▲] of crotonoyl CoA in the presence of 100 μM of NADH and various concentration of compound **6**. K_i was calculated from the X-intercept of Dixon plot assuming uncompetitive kinetics. Each data point represents the three independent sets of experiments.

Table 1
Inhibitory potencies of bromobenzothiphene derivatives against purified PfENR

Compound	Structure	Inhibition of PfENR ($IC_{50}\mu M$)
Triclosan	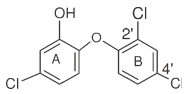	0.089 ± 0.005
2	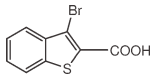	1.68 ± 0.045
4	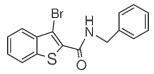	0.501 ± 0.033
5	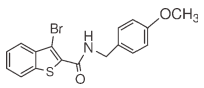	31.99 ± 0.23
6	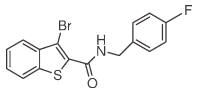	0.115 ± 0.012
7	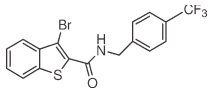	0.463 ± 0.01
8	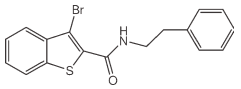	54.98 ± 0.42
9	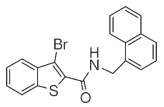	52.56 ± 0.33
10	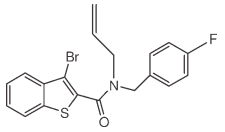	51.98 ± 0.43
11	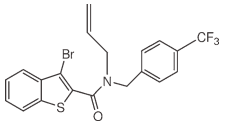	52.48 ± 0.22

$$\frac{1}{v} = \frac{k_m \times [I]}{V_{max} \times K_i \times [S]} + \frac{1}{V_{max}\left(1 + \frac{K_m}{[S]}\right)} \quad (1a)$$

$$\frac{1}{v} = \frac{[I]}{V_{max} \times K_i} + \frac{1}{V_{max}\left(1 + \frac{K_m}{[S]}\right)} \quad (1b)$$

Time dependent reversible inhibition can be described by any of the two mechanisms described later (*39*). In both the mechanisms, it is presumed that the slow binding inhibition step is reversible.

$$E + I \underset{k_4}{\overset{k_3}{\leftrightarrow}} E.I \qquad \text{(Mechanism 1)}$$

$$E + I \underset{k_4}{\overset{k_3}{\leftrightarrow}} E.I \overset{k_5}{\underset{k_6}{\leftrightarrow}} E.I^* \qquad \text{(Mechanism 2)}$$

The biphasic progress curves which are typical for slow tight binding inhibition were fitted to Eq. (2a) (*40, 41*) using nonlinear least squares fitting procedure. Corrections were made for the variation of the steady-state velocity with the inhibitor concentrations using Eqs. (2b) and (2c) (*40, 41*) as described earlier by Morrison and Walsh (*40, 41*).

$$P = v_s \times t + \frac{(v_o - v_s)[1 - \exp(-k_{obs} \times t)]}{k_{obs}} + C \quad (2a)$$

$$v_s = \frac{k_7 S Q}{2(K_m + S)} \quad (2b)$$

$$Q = [(K_i' + I_t - E_t) + 4K_i' E_t]^{1/2} - (K_i' + I_t - E_t) \quad (2c)$$

k_7, is the rate constant of the product formation $[E + S \underset{k_2}{\overset{k_1}{\leftrightarrow}} ES \overset{k_7}{\leftrightarrow} E + P]$.

The relationship between K_i, k_5, k_6, and k_{obs} is described in Eq. (3).

$$k_{obs} = k_6 + k_5 \left(\frac{\frac{1}{K_i}}{1 + \left(\frac{[S]}{K_m}\right) + \left(\frac{[I]}{K_i}\right)} \right)$$

RESULTS AND DISCUSSION

The elongation cycle of type II FAS involves four successive reactions: decarboxylative condensation to condense the growing acyl chain with malonyl-ACP by β-ketoacyl-ACP synthase (FabF), NADPH dependent reduction by β-ketoacyl-ACP reductase (FabG), dehydration by β-hydroxyacyl-ACP dehydratase (FabA or FabZ), and NADH dependent reduction by enoyl-ACP reductase (FabI or PfENR) (*9, 14–18*). All these enzymes have thioester substrates. Bromo-benzothiophene carboxamide derivatives have amide linkage in the midst of nonpolar moieties on either side which mimics the thioester linkage of the substrate. Therefore, the bromo-benzothiophene derivatives were tested against purified FabF, FabG, FabZ, and FabI. The compounds did not inhibit any other enzymes of the elongation cycle of malaria parasites fatty acid synthesis, namely FabF, FabG, and FabZ excepting PfENR. Aldose reductase an NADPH dependent oxidoreductase or alcohol dehydrogenase an NAD dependent enzyme were not inhibited by compound **6**, the best inhibitor of

Table 2
Dissociation constant, isomerization rate constant, dissociation rate constant of compounds **6** and **7** against purified PfENR

Compounds	Dissociation constant (K_i) nM	Isomerization rate constant ($k_5 \times 10^{-2}$) (s^{-1})	Dissociation rate constant ($k_6 \times 10^{-3}$) (s^{-1})
6	48.87	1.19 ± 0.045	1 ± 0.0004
7	86.1	1.65 ± 0.023	6.9 ± 0.0003

PfENR. These compounds thus inhibit FabI in specific manner. Other features of PfENR inhibition like (1) at least one of the rings in the inhibitors participate in Π–Π stacking interactions with the nicotinamide ring of the cofactor NADH and (2) the compound forms a hydrogen bond with the active site residue, tyrosine, are also satisfied by these compounds (*26, 29*). Docking studies discussed later further revealed optimum interactions between these compounds and PfENR.

To improve the efficacy of these compounds, bromo-benzothiophene carboxamide core was further derivatized with benzyl group attached *via* biodegradable amide (CONH) linkage. Incorporation of amide linkage improved the efficacy of the compound (compound **2**) marginally. Toward this end, benzyl group was further derivatized with various substituents like aromatic groups, halogens, and alkyl groups. We observed that fluoro derivatives (compounds **4**, **6**, and **7**) have significant improvement in their efficacy compared with other derivatives.

Docking of Benzothiophene Derivatives with PfENR

Docked conformations of bromo-benzothiophene carboxamide derivatives to PfENR reveal that these molecules occupy the hydrophobic pocket composed of Tyr 267, Ala 272, Tyr277, Gly 313, Pro 314, Phe 368, and Ile 369. Benzyl group is observed to be surrounded by substrate binding loop residues Ala 319, Ala 320, and Ile 323 and another loop from Ala 217 to Val 222. Amide group mimics the thioester of the substrate. Compound **6** has two hydrogen bonding interactions, 28 hydrophobic interactions, 16 aromatic–aromatic interactions, and 12 hydrophobic–hydrophilic interactions (Fig. 1a; Supporting Information Tables 1 and 2). There are 89 other interactions which are predominantly van der Waals interactions. Compound **6** also has extensive van der Waal's interaction with NAD^+. Benzyl ring of compound **6** makes Π–Π stacking interaction with nicotinamide ring of NAD^+. Its carbonyl group interacts with N7 group of NAD^+. Compound **7** has six hydrogen bonding interactions, 29 hydrophobic interactions, 18 aromatic–aromatic interactions and five hydrophobic–hydrophilic interactions (Fig. 1b; Supporting Information Tables 1 and 3). There are 99 other interactions mostly van der Waals type. Compound **7** also has extensive van der Waal's interaction with NAD^+ as well as Π–Π stacking interaction with nicotinamide ring of NAD^+.

Table 3
Inhibitory potencies of compound **6** against purified PfFAS enzymes

Enzymes	Inhibition at 10 M
PfFabF	No inhibition
PfFabG	No inhibition
PfFabZ	No inhibition
PfFabI	99%
ALR2	<1%
ADH	No inhibition

Kinetics of the Inhibition of PfFAS Enzymes

PfENR activity was determined using standard assay described earlier (*37*). The IC_{50} of the three best compounds were in nanomolar range and the remaining compounds were active at micromolar concentrations (Figs. 2a and 2b, Table 1). Compound **6** (IC_{50} = 0.115 ± 0.12 μM) was found to be most potent. The IC_{50} of other two potent compounds were also in

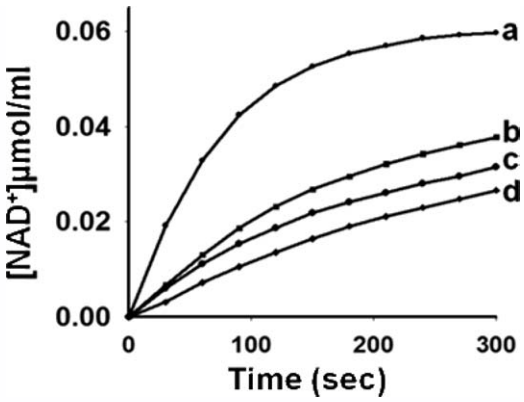

Figure 3. Potency assay of compound **6** for PfENR. The potency assay of compound **6** shows the slow onset of inhibition of PfENR by **6**. Curve "a" is control reaction without compound **6** but contained 1% DMSO, curve "b" is inhibition reaction in the presence of 115 nM of compound **6**, curve "c" shows further potentiation of inhibition when compound **6** was pre incubated with 35 nM of PfENR for 20 min, curve "d" is the inhibition reaction by compound **6** when 10 μM of NAD^+ was added to the preincubated mixture. The y-axis represents the accumulation of product NAD^+ in mM concentration with respect to time (in seconds, x-axis).

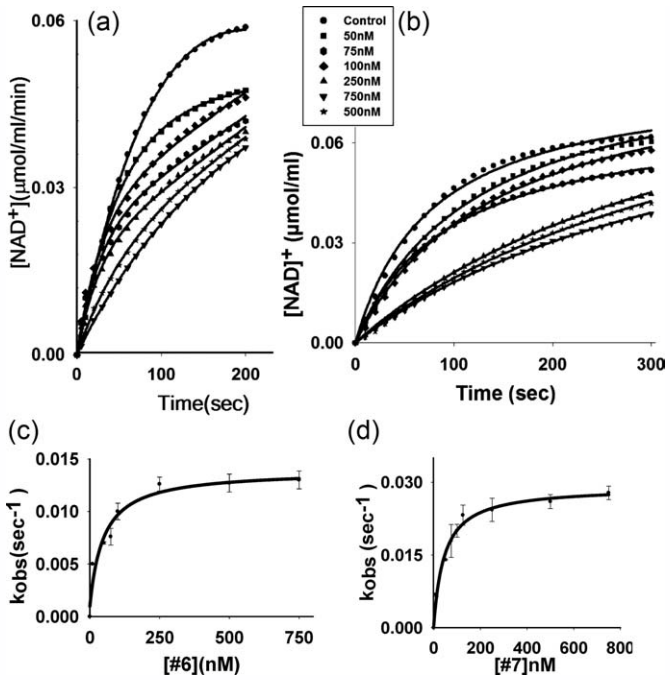

Figure 4. (a, b) Progress curves of compounds. For each concentration of compounds, progress curve was generated using Eq. (2a). In the control, standard reaction was set (as described in Experimental Section), and contained 1% DMSO apart from other constituents. Compounds were added in the reaction mixtures at various concentration (0–750 nM) as indicated in figure. The y-axis represents the accumulation of product NAD^+ in mM concentration with respect to time (in sec, x-axis). (a) Compound **6** and (b) compound **7**. (c, d) Dependence of PfENR inhibition on different concentrations of compounds. The initial inhibition rate constant (k_{obs}) (y-axis) for each compound concentration added was calculated from the progress curves using Eq. (2a). The k_{obs} thus calculated were fitted to Eq. (3) with respect to respective concentrations of each compound and the best fit gave hyperbolic curve demonstrating two phase inhibition mechanism. The error bars represents the standard deviation of the data. (c) Compound **6** and (d) compound **7**.

the nanomolar range (Compounds **7** = 0.463 ± 0.1 µM, **2** = 0.51 ± 0.33 µM). K_i values for the best inhibitor, compound **6** were determined individually against cofactor NADH and substrate crotonoyl CoA. It gave competitive kinetics with NADH and uncompetitive against crotonoyl CoA (Figs. 2c and 2d). The K_i values are indicated in Table 2. Compound **6** was shown to have IC_{50} more than 100 µM against other purified FAS enzymes (Table 3). Analysis of kinetic data showed that these inhibitors compete with NADH for binding to PfENR.

Cofactor Potency Assays

NAD^+ was shown to potentiate the binding of compound **6** to PfENR (Fig. 3) (*38*). The control reaction showed a linear increase in the accumulation of NAD^+ (curve a), whereas when the reaction was carried out in the presence of compound **6**, accumulation of product decreased (curve b). The accumulation of product further decreased when compound **6** was preincubated with the enzyme (curve c). On addition of NAD^+ to this reaction the rate of product accumulation further decreased (curve d). This also indicated that these are slow tight binding inhibitors of PfENR.

Detailed Analysis of the Progress Curves of Bromo-benzothiophene Carboxamide Derived Inhibitors for PfENR

Progress curves for inhibition by varying concentrations of compounds **6** and **7** were examined in detail (Figs. 4a and 4b). From the progress curve analyses, it was adjudged that for each concentration of the inhibitors the initial and the steady state velocity decreased exponentially with time. At higher inhibitor concentration, steady state is reached rapidly with a decrease in steady state velocity (v_s). It indicates that initially a loose complex of inhibitor, NAD^+, and PfENR is formed which slowly isomerises into a more stable tight complex.

Progress curves were analyzed using Eq. (3a) from which a series of K_{obs} values were obtained for each concentration of inhibitor. The determined K_{obs} values were plotted against respective concentrations of compounds **6** and **7** which resulted in hyperbolic curve (Figs. 4c and 4d). Hyperbolic curve indicated biphasic binding of inhibitors again reflecting slow tight binding behavior of bromo-benzothiophene carboxamide derived inhibitors of PfENR (*40, 41*).

CONCLUSIONS

De novo fatty acid synthesis in the malaria parasites either provide unique fatty acids or its role is to augment levels of salvaged fatty acids (from host) to meet the huge demand during their growth phase. In either case, disruption of the *de novo* synthesis in parasites, by inhibitor(s), is an attractive target. Bromo-benzothiophene carboxamide compounds specifically inhibit PfENR and not the other enzymes of FASII elongation module, NADPH dependent aldose reductase, or NAD alcohol dehydrogenase. Compounds **6** and **7** inhibited PfENR with an IC_{50} of 115 nM and 463 nM, respectively, proving that PfENR is a key target of these compounds and were found to be slow tight binding inhibitors of PfENR. Hence these compounds hold promise to be significant antimalarials.

ACKNOWLEDGEMENTS

The authors thank the Department of Biotechnology, Government of India, for the grant to N.S. and A.S. as well as Centre of Excellence grant to A.S. N.S. holds TATA Innovation fellowship of the Department of Biotechnology, Government of India. T.B. and S.K.S. thank the Council of Scientific and

Industrial Research, Government of India for Senior Research fellowship.

REFERENCES

1. Peters, W. (1998) Drug resistance in malaria parasites of animals and human. *Adv. Parasitol.* **41**, 1–62.
2. Krogstad, D. J., Gluzman, I. V., Kyle, D. E., Oduola, A. M. J., Martins, S. K., Milhouse, W. K., and Schlesinger, P. H. (1987) Efflux of chloroquine from *Plasmodium falciparum*: mechanism of chloroquine resistance. *Science* **238**, 1283–1285.
3. Bray, P. G., Mungthin, M., Riley, R. G., and Ward, S. A. (1998) Access to hematin the basis of chloroquine resistance. *Mol. Pharmacol.* **54**, 170–179.
4. Mutabingwa, T. K., Anthony, D., Heller, A., Hallett, R., Ahmed, J., et al. (2005) Amodiaquine alone, amodiaquine + sulfadoxine-pyrimethamine, amodiaquine + artesunate, and artemether-lumefantrine for outpatient treatment of malaria in Tanzanian children: a four-arm randomised effectiveness trial. *Lancet* **365**, 1474–1480.
5. Rathod, P. K., McErlean, T., and Lee, P. C. (1997) Variations in the frequencies of drug resistance in *Plasmodium falciparum*. *Proc. Natl. Acad. Sci. USA* **94**, 9389–9393.
6. WHO. 1999. Rolling back malaria. In: The World Health Report 1999: making a difference. Geneva. Switzerland. pp. 49–63.
7. Smith, S., Witkowski, A., and Joshi, A. K. (2003) Structural and functional organization of the animal fatty acid synthase. *Prog. Lipid Res.* **42**, 289–317.
8. Ralph, S. A., Van Dooren, G. G., Waller, R. F., Crawford, A. F., Fraunholz, M., et al. (2004) Metabolic maps and functions of the *Plasmodium falciparum* apicoplast. *Nat. Rev. Microbiol.* **2**, 203–216.
9. Rock, C. O. and Cronan, J. E. (1996) *Escherichia coli* as a model for the regulation of dissociable (type II) fatty acid biosynthesis. *Biochim. Biophys. Acta* **132**, 1–16.
10. Surolia, N. and Surolia, A. (2001) Triclosan offers protection against blood-stages of malaria by inhibiting enoyl-ACP reductase of *Plasmodium falciparum*. *Nat. Med.* **7**, 167–173.
11. Heath, R. J. and Rock, C. O. (2004) Fatty acid biosynthesis as a target for novel antibacterials. *Curr. Opin. Investig. Drugs* **5**, 46–53.
12. Singh, A. P., Surolia, N., and Surolia, A. (2009) Triclosan inhibit the growth of the late liver-stage of *Plasmodium*. *IUBMB Life*. **61**, 923–928.
13. Vaughan, A. M., O'Neill, M. T., Tarun, A. S., Camargo, N., Phuong, T. M., et al. (2009) Type II fatty acid is essential for only late liver-stage development. *Cell. Microbiol.* **11**, 506–520.
14. Mahmoudi, N., Ciceron, L., Franetich, J. F., Farhati, K., Silvie, O., et al. (2003) *In vitro* activities of 25 quinolones and fluoroquinolones against liver and blood-stage *Plasmodium* spp. *Antimicrob. Agents Chemother.* **47**, 2636–2639.
15. Surolia, A., Ramya, T. N. C., Ramya, V., and Surolia, N. (2004) 'FAS't inhibition of malaria. *Biochem. J.* **383**, 410–412.
16. Chhibber, M., Kumar, G., Parasuraman, P., Ramya, T. N., and Surolia, N., Surolia, A. (2006) Novel diphenyl ethers: design, docking studies, synthesis, and inhibition of enoyl ACP reductase of *Plasmodium falciparum* and *Escherichia coli*. *Bioorg. Med. Chem.* **14**, 886–898.
17. Kumar, S., Kumar, G., Kapoor, M., Surolia, A., and Surolia, N. (2006) Synthesis and evaluation of substituted pyrazoles: potential anti-malarials targeting the enoyl ACP reductase of *Plasmodium falciparum*. *Synth. Commun.* **36**, 215–226.
18. Sharma, S. K., Prasanna, P., Kumar, G., Surolia, N., and Surolia, A. (2007) Green tea catechins potentiate triclosan binding to enoyl-ACP reductase from *Plasmodium falciparum* (PfENR). *J. Med. Chem.* **50**, 765–775.
19. Malamas, M. S., Sredy, J., Moxham, C., Katz, A., Xu, W., et al. (2000) Novel benzofuran and benzothiophene biphenyls as inhibitors of protein tyrosine phosphatase 1B and antihyperglycemic properties. *J. Med. Chem.* **43**, 1293–1310.
20. Qin, Z., Kastrati, I., Ashqodom, R. T., Lantvit, D. D., Overk, C. R., et al. (2009) Structural modulation of oxidative metabolism in design of improved benzothiophene selective estrogen receptor modulators. *Drug Metab. Dispos.* **37**, 161–169.
21. Bolognese, M., Krege, J. H., Utian, W. H., Feldman, R., Broy, S., et al. (2009) Effects of arzoxifene on bone mineral density and endometrium in post menopausal women with normal or low bone mass. *J. Clin. Endocrinol. Metab.* **94**, 2284–2289.
22. Thorneloe, K. S., Sulpizio, A. C., Lin, Z., Fiqueroa, D. J., Clouse, A. K., et al. (2008) N-((1S)-1-{[4-((2S)-2-[(2,4-Dichlorophenyl)sulfonyl]amino}-3-hydroxypropanoyl)-1-piperazinyl]carbonyl}-3-methylbutyl)-1-benzothiophene-2-carboxamide (GSK116790A), a novel and potent transient receptor potential vanilloid 4 channel agonist induces urinary bladder contraction and hyperactivity. Part I. *J. Pharmacol. Exp. Ther.* **326**, 432–442.
23. Villar, R., Encio, I., Miqliaccio, M., Gil, M. J., and Martinez-Merino, V. (2004) Synthesis and cytotoxic activity of lipophillic sulphonamide derivatives of the benzo[b]thiophene 1,1 dioxide. *Bioorg. Med. Chem.* **12**, 963–968.
24. Youngs, C. G., Epp, A., Craig, B. M., and Sallans, H. R. (1956) Preparation of long-chain fatty acid chlorides. *J. Am. Oil Chem. Soc.* **34**, 107–108.
25. Kim, K. S. and Kim, H. S. (2004) Molecular Tweezer based on chenodeoxycholic acid: synthesis and anion binding properties. *Bull. Korean Chem. Soc.* **25**, 1411–1413.
26. Pidugu, L. S., Kapoor, M., Surolia, N., Surolia, A., and Suguna, K. (2004) Structural basis for the variation in triclosan affinity to enoyl reductases. *J. Mol. Biol.* **343**, 147–155.
27. Molecular Operating Environment [MOE 201.7], Chemical Computing Group Inc., Montreal, Quebec, Canada, H3B 3X3.
28. Sobolev, V., Sorokine, A., Prilusky, J., Abola, E. E., and Edelmanm, M. (1999) Automated analysis of interatomic contacts in proteins. *Bioinformatics* **15**, 327–332.
29. Kapoor, M., Mukhi, P. L., Surolia, N., Suguna, K., and Surolia, A. (2004) Kinetic and structural analysis of the increased affinity of enoyl-ACP (acylcarrier protein) reductase for triclosan in the presence of NAD+. *Biochem. J.* **381**, 725–733.
30. Lack, G., Homberger-Zizzari, G., Folkers, G., Scapozza, L., and Perozzo, R. (2006) Recombinant expression and biochemical characterisation of the unique elongating beta-ketoacyl-acyl carrier protein synthase involved in fatty acid biosynthesis of *Plasmodium falciparum* using natural and artificial substrates. *J. Biol. Chem.* **281**, 9538–9546.
31. Karmodiya, K. and Surolia, N. (2006) Analyses of co-operative transitions in *Plasmodium falciparum* beta-ketoacyl carrier protein reductase upon co-factor and acyl carrier protein binding. *FEBS J.* **273**, 4093–4103.
32. Sharma, S. K., Kapoor, M., Kumar, S., Kumar, G., Modak, R., Sharma, S., Surolia, N., and Surolia, A. (2003) Identification, characterisation and inhibition of *Plasmodium falciparum* ß-hydroxyacyl-acyl carrier protein dehydratase (FabZ). *J. Biol. Chem.* **278**, 45661–45671.
33. Suguna, K., Surolia, A., and Surolia, N. (2001) Structural basis for triclosan and NAD binding to enoyl-ACP reductase of *Plasmodium falciparum*. *Biochem. Biophys. Res. Commun.* **283**, 224–228.
34. Petrash, J. M., Harter, T. M., Devine, C. S., Olins, P. O., Bhatnagar, A., Liu, S., and Srivastava, S. K. (1992) Involvement of cysteine residues in catalysis and inhibition of human aldose reductase: Site-directed mutagenesis of Cys-80, -298, and -303. *J. Biol. Chem.* **267**, 24833–24840.
35. Suryanarayana, P., Kumar, P. A., Saraswat, M., Petrash, J. M., and Reddy, G. B. (2004) Inhibition of aldose reductase by tannoid principles of Emblica officinalis: implications for the prevention of sugar cataract. *Mol. Vis.* **10**, 148–154.
36. Arslanian, M. J., Pascoe, E, and Reinhold, J. G. (1971) Rat liver alcohol dehydrogenase. Purification and properties. *Biochem. J.* **125**, 1039–1047.

37. Kapoor, M., Dar, M. J., Surolia, A., and Surolia, N. (2001) Kinetic determination of the interaction of enoyl-ACP reductase from *Plasmodium falciparum* with its substrates and inhibitors. *Biochem. Biophys. Res. Commun.* **289**, 832–837.
38. Kapoor, M., Reddy, C. C., Krishnasastry, M. V., Surolia, N., and Surolia, A. (2004) Slow-tight-binding inhibition of enoyl-acyl carrier protein reductase from *Plasmodium falciparum* by triclosan. *Biochem. J.* **381**, 719–724.
39. Dixon, M. (1972) The graphical determination of K_m and K_i. *Biochem. J.* **129**, 197–202.
40. Morrison, J. F. and Walsh, C. (1988) The behaviour and significance of slow tight binding enzyme inhibitors. *Adv. Enzymol. Relat. Areas Mol. Biol.* **61**, 21–31.
41. Morrison, J. F. (1982) The slow binding and slow tight binding inhibition of enzyme catalysed reactions. *Trends Biochem. Sci.* **7**, 12–15.